Calibration of an extreme-ultraviolet transmission grating spectrometer with synchrotron radiation

John F. Seely, Charles M. Brown, Glenn E. Holland, Frederick Hanser, John Wise, James L. Weaver, Raj Korde, Rodney A. Viereck, Richard Grubb, and Darrell L. Judge

The responsivity of an extreme-ultraviolet transmission grating spectrometer with silicon photodiode detectors was measured with synchrotron radiation. The spectrometer was designed to record the absolute radiation flux in a wavelength bandpass centered at 30 nm. The transmission grating had a period of 200 nm and relatively high efficiencies in the +1 and the −1 diffraction orders that were dispersed on either side of the zero-order beam. Three photodiodes were positioned to measure the signals in the zero order and in the +1 and −1 orders. The photodiodes had aluminum overcoatings that passed the desired wavelength bandpass centered at 30 nm and attenuated higher-order radiation and wavelengths longer than approximately 80 nm. The spectrometer's responsivity, the ratio of the photodiode current to the incident radiation power, was determined as a function of the incident wavelength and the angle of the spectrometer with respect to the incident radiation beam. The spectrometer's responsivity was consistent with the product of the photodiode responsivity and the grating efficiency, both of which were separately measured while removed from the spectrometer.

OCIS codes: 120.6200, 040.7480, 050.1950.

1. Introduction

Extreme-ultraviolet (EUV) spectrometers using transmission gratings and silicon photodiode detectors with thin metal coatings are planned for the next series of Geostationary Operational Environmental Satellites (GOES N, O, P, and Q). The spectrometers are designed to measure the absolute solar flux in four wavelength bandpasses that are established by the dispersion of the transmission gratings and the positions of the detectors. The thin metal coating on each detector transmits the wavelength bandpass of interest, attenuates shorter wavelengths that may fall on the detector in the higher diffraction orders of the grating, and blocks scattered longer-wavelength radiation. The GOES spectrometers have an additional fifth channel that measures the hydrogen Lyman-α flux at a wavelength of 121.6 nm by use of narrow-bandpass filters.

This type of transmission grating spectrometer was developed for a rocket mission to measure the absolute solar flux in a bandpass centered at a wavelength of 30 nm and approximately 8 nm in width.[1] The rocket spectrometer had a gold transmission grating with 5000 bars/mm. The three photodiode detectors, each with a 150-nm-thick aluminum coating, were positioned to measure the 30-nm bandpass in the +1 and the −1 diffraction orders and the broadband radiation in the zero order. An additional freestanding aluminum filter, 150 nm thick, covered the entrance aperture of the spectrometer. The wavelength responsivity of the zero-order detector was primarily established by the transmittance of the aluminum filter and the aluminum coating on the detector. The zero-order responsivity was relatively high at wavelengths longer than the aluminum L edge at 17 nm. The responsivity was also high at wavelengths shorter than 10 nm, where aluminum is transmissive.

A similar spectrometer, the solar EUV monitor (SEM), is currently flying on the Solar and Heliospheric Observatory (SOHO).[2] A spectrometer identical to the SOHO spectrometer was flown on several

J. F. Seely (john.seely@nrl.navy.mil), C. M. Brown, and J. L. Weaver are with the Space Science Division, Naval Research Laboratory, Washington, D.C. 20375. G. E. Holland is with SFA Inc., 1401 McCormick Drive, Landover Maryland 20785. F. Hanser and John Wise are with Panametrics Inc., 221 Crescent Street, Waltham, Massachusetts 02453. R. Korde is with International Radiation Detectors Inc., Torrance California 90505. R. A. Viereck and R. Grubb are with the National Oceanic and Atmospheric Administration, Boulder, Colorado 80303. D. L. Judge is with the Space Science Center, University of Southern California, Los Angeles, California 90089.

Received 13 September 2000; revised manuscript received 2 January 2001.

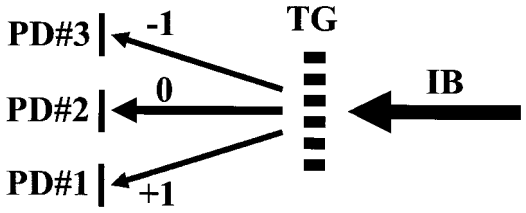

Fig. 1. Schematic of the spectrometer showing the incident beam (IB), the transmission grating (TG), the three photodiodes, and the 0 and the ±1 diffraction orders. The incident synchrotron radiation is polarized in the dispersion plane, with the electric field vector perpendicular to the grating bars.

rocket missions for the purpose of calibrating the SEM and the other instruments on SOHO.[3]

The currently calibrated spectrometer is similar to the SEM,[2,3] except that an aluminum entrance aperture filter is not used. As shown in Fig. 1, the spectrometer consists of a transmission grating with 5000 bars/mm and three aluminum-coated silicon photodiodes. Photodiode 2 (PD#2) is positioned on the axis of the spectrometer to record the broadband radiation in the zero diffraction order. PD#1 and PD#3 are positioned symmetrically on either side of the spectrometer axis and record the 30-nm bandpass in the +1 and the −1 orders, respectively.

The spectrometer's responsivity, the ratio of the photodiode current and the incident radiation power, was measured as a function of wavelength with EUV synchrotron radiation. Afterward, the efficiency of the transmission grating and the responsivities of the three aluminum-coated photodiodes were measured while removed from the spectrometer. The measurements were performed with beamline X24C at the National Synchrotron Light Source.

Compared with the previous calibrations of similar spectrometers that were performed at the Synchrotron Ultraviolet Radiation Facility (SURF) synchrotron at the National Institutes of Standards and Technology (NIST),[1–3] the present measurements extend to shorter wavelengths (2.8 nm compared with 5 nm) where aluminum is increasingly transmissive. These measurements more accurately determine the responsivity of the spectrometer's zero-order channel (PD#2) to soft x rays that, in the case of broadband solar illumination, tend to obscure the responsivity at longer wavelengths above the aluminum L edge at 17 nm. In addition, the shifts in the wavelength coverages of PD#1 (+1 order) and PD#3 (−1 order) resulting from off-axis illumination were measured.

The spectrometer's entrance aperture was established by the frame that held the transmission grating. The aperture was 4 mm wide and 10 mm high. The transmission grating was oriented with its bars vertical, parallel to the 10-mm dimension of the aperture. It was necessary to measure the size and divergence of the incident radiation beam to verify that the beam underfilled the spectrometer aperture and underfilled the photodiode detectors when the spectrometer was centered on the incident beam.

The distance from the transmission grating to the detector plane was 200 mm. One photodiode detector (PD#2 in Fig. 1) was mounted on the axis of the spectrometer. The other two detectors (PD#1 and PD#3) were mounted with their centers at a distance of 30.4 mm from the spectrometer axis. An aperture covered each detector and was 5.9 mm wide and 15.9 mm high.

2. Incident Synchrotron Radiation Beam

The size and intensity profile of the incident radiation beam was characterized by use of silicon photodiodes with circular or slit apertures. The photodiodes were of the type AXUV-100G that have a thin (6-nm) SiO_2 surface dead layer and good sensitivity in the ultraviolet, EUV, and soft-x-ray regions.[4,5] These photodiodes have negligible surface recombination losses and thermal nitridation that provides a stable surface layer.[6–8] Owing to the reproducibility of the lithographic fabrication process, the well-understood optical properties of silicon, and the excellent stability of the detectors, responsivity calibration models were developed that depend primarily on the physical design of the detector regions and the carrier collection efficiency in each region.[9–12]

The measurements were performed at the National Synchrotron Light Source with the Naval Research Laboratory beamline X24C.[13,14] The synchrotron radiation was dispersed by a grating monochromator that had a resolving power of 600. Thin filters attenuated the radiation from the monochromator in the higher harmonics of the diffraction grating. The beam-profile measurements were performed at a wavelength of 29.5 nm with an aluminum–magnesium–aluminum filter with layer thicknesses of 32.2, 263.5, and 32.2 nm, respectively. This filter had good transmittance in the 25–50-nm-wavelength working range established between the first- and the second-order appearances of the magnesium L_{III} edge at 24.8 nm. The two outer aluminum layers also prevent oxidation of the center magnesium layer.

The monochromator exit slit, which was in the horizontal direction, was set to a width of 400 μm, which provided reasonably large photodiode signals and small vertical beam divergence. A beamline baffle was set to its minimum horizontal width, which resulted in minimum horizontal beam divergence. At a wavelength of 29.5 nm and with the aluminum–magnesium–aluminum filter, the current measured by a precision Keithley electrometer was 16.8 nA. On the basis of the calibrated responsivity (0.22 A/W) of the AXUV-100G photodiode at a wavelength of 29.5 nm that was provided by NIST,[15] the incident photon flux was 2.8×10^{11} photons/cm^2 s. This was approximately an order of magnitude larger than the photon flux used for the SURF measurements.[1] By comparison, the detector's dark current was typically 3 pA.

Shown in Fig. 2(a) is the radiation beam profile measured at a distance of 130 cm in front of the transmission grating and 40 cm downstream of the monochromator exit slit. The profile was measured by means of scanning an AXUV-100G detector with a

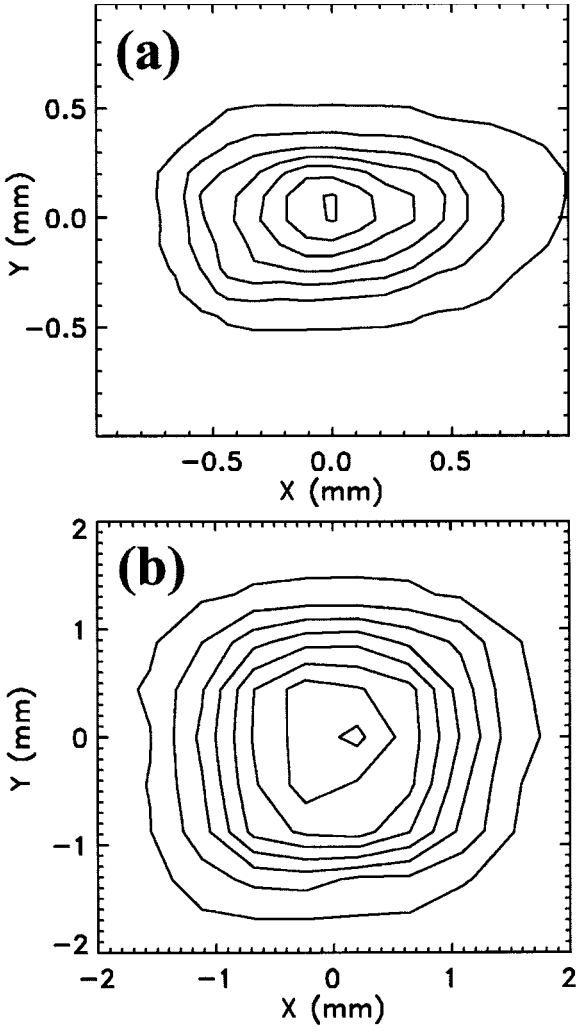

Fig. 2. Intensity profile of the incident beam (a) at a distance of 130 cm in front of the spectrometer's transmission grating and (b) at the position of the transmission grating. The incident wavelength was 29.5 nm. The X direction is horizontal, and the Y direction is vertical. The contour values are (a) 0.01, 0.04, 0.07, 0.10, 0.13, 0.16, and 0.19 and (b) 0.1, 0.3, 0.5, 0.7, 0.9, 1.1, 1.3, and 1.5.

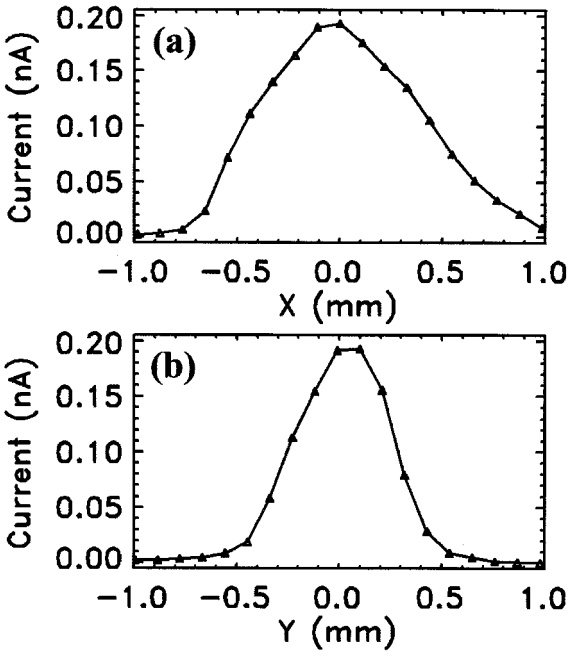

Fig. 3. Relative incident beam intensity in (a) the horizontal direction and (b) the vertical direction at a distance of 130 cm in front of the spectrometer's transmission grating. The data points were derived by means of stepping a detector with a 150-μm circular aperture through the incident beam. The incident wavelength was 29.5 nm.

150-μm-diameter aperture through the beam in 109-μm increments in the horizontal (X) and vertical (Y) directions. Shown in Fig. 3(a) is the beam profile in the horizontal direction derived by summation of the data in the vertical direction. The corresponding beam profile in the vertical direction is shown in Fig. 3(b). The width and the height of the beam at the half-maximum levels are approximately 0.9 and 0.6 mm, respectively.

The beam profile measured at the position of the transmission grating is shown in Fig. 2(b). The profile was measured by means of scanning a detector with a 570-μm-diameter aperture through the beam in 440-μm steps. The horizontal and the vertical beam profiles, derived by summation of the data, are shown by the large square data points in Fig. 4. Also shown in Fig. 4 (small triangular data points) are the horizontal and the vertical profiles measured by means of scanning detectors with 100-μm vertical or horizontal slits with 88-μm steps. The beam width and height at the half-maximum levels are 2.0 and 2.1 mm, respectively.

From the beam profiles measured at the grating position and at a distance of 130 cm upstream, the inferred beam divergence is ±0.4 mrad in the horizontal direction and ±0.6 mrad in the vertical direction. We conclude that the beam was smaller than the spectrometer's entrance aperture (4 mm wide and 10 mm high) and also that the beam was smaller than the spectrometer's detector apertures (5.9 mm wide and 15.9 mm high). We verified this by moving the spectrometer through the radiation beam while keeping the spectrometer axis parallel to the beam. The currents from spectrometer PD#2 (zero order) for the vertical and the horizontal scans are shown in Figs. 5(a) and 5(b). In both cases the data are consistent with the beam and aperture sizes. That is, the current rises (and falls) over a distance of approximately 1.5 mm (consistent with Fig. 4), and the horizontal and the vertical scans shown in Figs. 5(a) and 5(b) have narrow and wide flat regions, respectively, near the spectrometer axis. The flat region of the vertical scan also indicates that the responsivity of the aluminum-coated PD#2 and the zero-order grating efficiency are uniform in the vertical direction to within 4%.

After the beam was centered in the spectrometer's entrance aperture, the spectrometer was rotated in the horizontal plane about a vertical axis through the

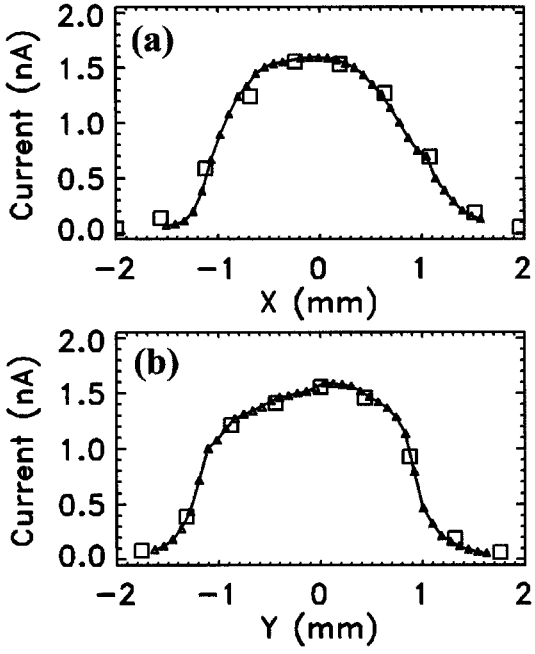

Fig. 4. Relative incident beam intensity in (a) the horizontal direction and (b) the vertical direction at the position of the spectrometer's transmission grating. The small triangular data points were obtained by means of stepping detectors with 100-μm-wide slit apertures through the incident beam. The large square data points were derived by means of stepping a detector with a 570-μm circular aperture through the incident beam. The incident wavelength was 29.5 nm.

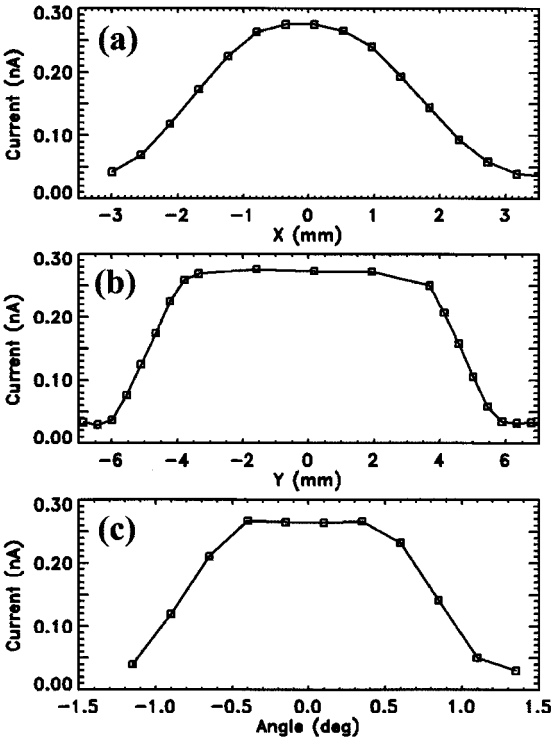

Fig. 5. Zero-order signal measured when the spectrometer was moved across the incident beam in (a) the horizontal direction and (b) the vertical direction. (c) is the signal measured when the spectrometer was rotated with respect to the incident beam. The incident wavelength was 29.5 nm.

center of the grating. The current from PD#2 is shown as a function of angle in Fig. 5(c). Considering that the detector is 200 mm from the axis of rotation, the data are consistent with the 1.7° angular width of the 5.9-mm detector aperture and the 0.6° effective angular width of the 2.0-mm beam.

3. Transmission Grating

The transmission grating consisted of gold bars with a period of 200 nm.[16] The fine-grating gold bars were supported by a coarse gold-bar mesh that, in the absence of the fine-grating bars, would transmit approximately 40% of the incident radiation.

The transmission grating, after removal from the spectrometer, was mounted in a rotational fixture in an EUV synchrotron reflectometer.[13,14] The detector in the reflectometer was mounted on a rotating arm that traveled in a circle nearly 360° around the sample at its center. The detector could measure the incident beam (when the sample was removed) or the beams that were transmitted or reflected by the sample.

The plane of the grating was perpendicular to the incident beam. The incident beam was approximately 80% polarized with the electric field vector in the horizontal plane and perpendicular to the gold bars of the transmission grating. An AXUV-100G detector was rotated in angle through the diffraction orders. The efficiency was calculated by means of dividing the detector current by the current measured when the transmission grating was removed from the radiation beam. The efficiencies measured at incident wavelengths of 8.86 and 30.4 nm are shown in Fig. 6. The 0.5° angular width of the orders was determined by the 1-mm-wide slit that covered the detector. The average efficiency in the ± 1 orders at a wavelength of 8.86 nm is 3.3%, and the efficiencies in the higher orders are much lower. On the basis of modeling the transmission grating efficiency, the low efficiency in the higher orders indicates that the width of the gold bars was approximately equal to the width of the open channels between the gold bars. In Fig. 6 there is no evidence of higher harmonic radiation from the monochromator, which if present would appear at angular positions corresponding to fractional orders of <1.

The peak efficiencies in the diffraction orders 0–3 that were derived from the detector angular scans at a number of incident wavelengths from 2.88 to 47.7 nm are shown in Fig. 7, where straight lines are drawn between the square data points. In general, the efficiencies tend to decrease at the longer wavelengths as expected from the waveguide cutoff condition.[17]

4. Silicon Photodiodes

The spectrometer's silicon photodiode detectors had aluminum coatings that were designed to transmit

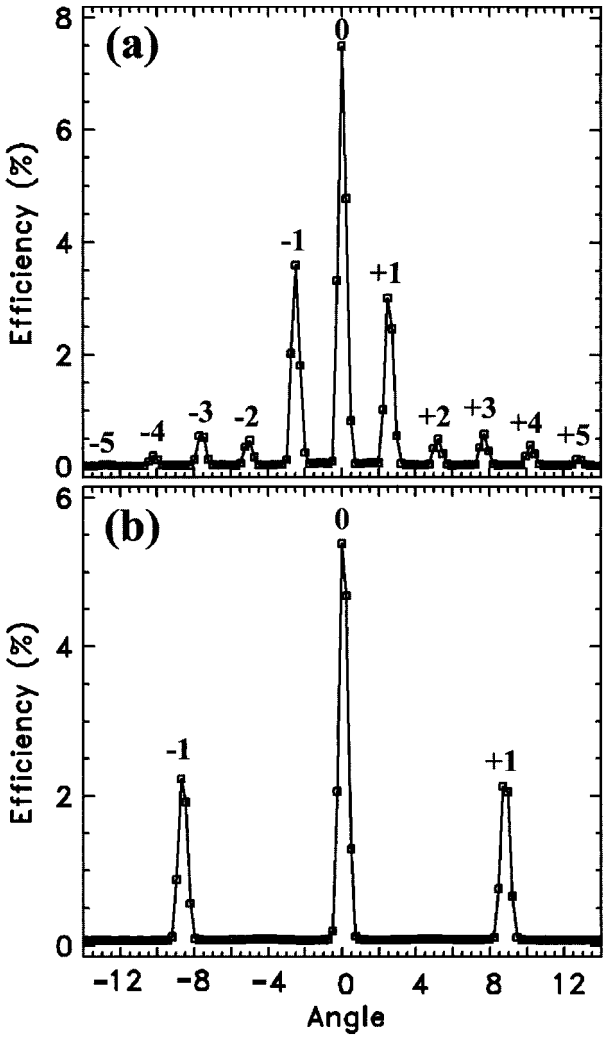

Fig. 6. Transmission grating efficiency measured for incident wavelengths of (a) 8.86 nm and (b) 30.4 nm. The diffraction orders are indicated.

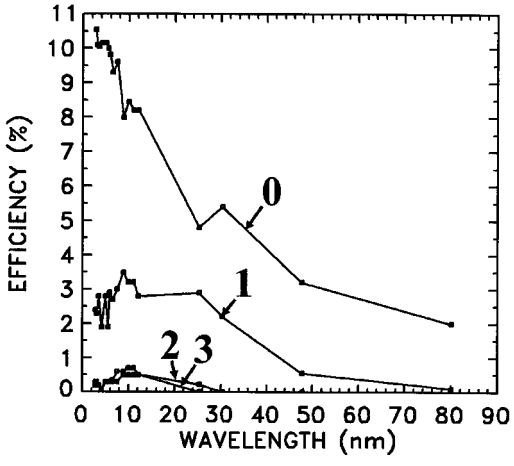

Fig. 7. Peak efficiencies in the indicated orders that were derived from the detector angular scans at fixed incident wavelengths. Straight lines were drawn between the data points.

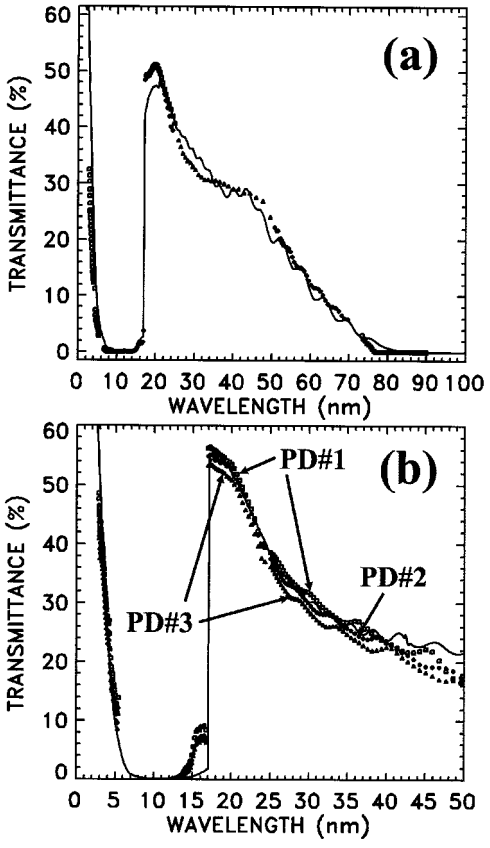

Fig. 8. (a) Measured transmittance of an aluminum coating on a photodiode (data points) and the calculated transmittance of an aluminum coating with 200 nm thickness (curve). (b) The measured (data points) and the calculated (curve) transmittances of the aluminum coatings on the spectrometer's three photodiodes.

the 30-nm radiation of interest and to block the longer-wavelength ultraviolet and visible radiation. The transmittance of a typical aluminum coating is shown by the data points in Fig. 8(a). The measured quantity was the ratio of the current from the aluminum-coated detector divided by the current from an uncoated AXUV-100G reference detector at the same incident wavelength. This ratio is effectively the transmittance of the aluminum coating. The detector currents were measured by means of scanning the incident wavelength over six wavelength ranges from 2.7 to 100 nm. An appropriate beamline filter was used to attenuate higher harmonic radiation from the monochromator in each wavelength range.

The curve in Fig. 8(a) is the calculated effective transmittance for an aluminum thicknesses of 190 nm. It was assumed that the aluminum coating had a additional 10-nm-thick Al_2O_3 layer on the surface. The effective transmittance was calculated with an optical model.[18] This model solved the boundary value problem of an electromagnetic field propagating through the layers of the coating and the underlying photodiode regions. The model accounted for the optical properties of each layer of the coating and the photodiode, the polarization of the incident radi-

ation, the reflectance and transmittance at the boundaries, and the attenuation of the field strength in the layers. The responsivities of the coated photodiode and the uncoated reference photodiode were calculated on the basis of energy deposition and the carrier collection efficiency in each coating layer and photodiode region. The optical constants for Al_2O_3, aluminum, and silicon were from Refs. 19 and 20.

As shown in Fig. 8(a), the effective transmittance of the aluminum coating is low at wavelengths below the aluminum L_{III} absorption edge at 17.1 nm. The aluminum coating becomes more transmissive again at wavelengths below 10 nm. The transmittance is negligible for wavelengths longer than 80 nm. In the case of broadband illumination of the spectrometer, the detector's aluminum coating transmits the desired wavelength bandpass centered at 30 nm, attenuates the shorter wavelengths that fall on the detector in the second through fifth diffraction orders of the transmission grating, and blocks scattered radiation with wavelengths longer than 80 nm.

The transmittances of the aluminum coatings on the spectrometer's three photodiodes were measured after removal from the spectrometer. The measured transmittances are shown by the data points in Fig. 8(b). The curve in Fig. 8(b) is the calculated transmittance for 200-nm-thick aluminum and 12.5-nm-thick Al_2O_3.

The light-blocking performance of the aluminum-coated photodiodes was determined by illumination of the photodiodes with the zero-order beam from the monochromator. A sapphire window was inserted into the beam, which attenuated wavelengths shorter than 140 nm. The current from the uncoated reference photodiode was 1.56 μA, and the currents from the aluminum-coated photodiodes were at the background-noise level of 3 pA. Thus the measured lower limit on the blocking factor for radiation with wavelengths longer than 140 nm was 5×10^5.

The uniformity of the responsivities of the aluminum-coated photodiodes was determined by means of moving the photodiodes relative to the incident beam. At an incident wavelength of 20 nm, the current varied by less than ±0.8%.

In some cases, depending on the mounting of the photodiode, photoelectrons may be generated and collected by the external circuit. This may occur in wavelength regions where the photodiode's surface layer is highly absorbing and the photoelectrons are generated near the surface. In this case the photoelectrons have a higher probability of escape from the surface and collection by the external circuit. However, the aluminum coating is sufficiently transmissive in the 30-nm region that the current resulting from photoelectrons is negligible.

5. Spectrometer Responsivity

The spectrometer was characterized in the following manner. The spectrometer axis was oriented parallel to the incident radiation beam, and the dispersion direction was horizontal. The spectrometer was moved perpendicular to the beam so that the zero-order beam was centered on PD#2 (see Fig. 1). The incident wavelength from the monochromator was scanned while the currents were recorded from the three detectors. At each incident wavelength the spectrometer detector currents were divided by the current from the AXUV-100G reference detector that was placed in the incident beam.

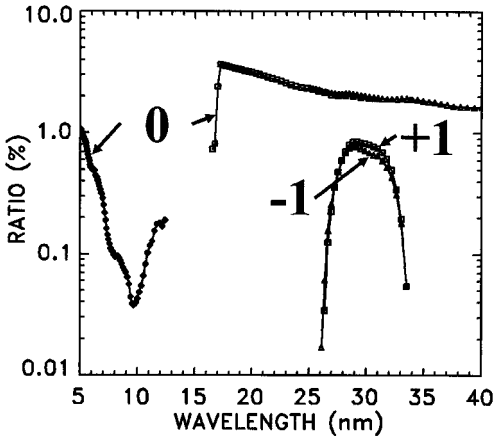

Fig. 9. Relative I/I_o signals measured in the zero diffraction order by PD#2, the +1 order by PD#1, and the −1 order by PD#3.

The measured current ratios are shown in Fig. 9. The wavelength dependence of the zero-order data is determined primarily by the transmittance of the aluminum coating on PD#2 [Fig. 8(b)] and by the zero-order grating efficiency (Fig. 7). The +1 order measured by PD#1 and the −1 order measured by PD#3 are lower, owing to the lower ±1 efficiencies as compared with zero order (Fig. 7).

The wavelength dependence of the ±1 orders in Fig. 9 results from the change in the angle of diffraction with wavelength. For the case of a grating with normal-incidence illumination, the grating equation is $n\lambda = d \sin \beta$ where d is the grating period and β is the angle of diffraction. The wavelength interval subtended by the detector is $\delta\lambda \approx d\delta\beta$ where $\delta\beta \approx W/D$, W is the width (5.9 mm) of the detector aperture, and D is the detector-to-grating distance (200 cm). When we neglect the size of the dispersed beam, the wavelength interval subtended by PD#1 and PD#3 is approximately 6 nm.

The currents from PD#1 and PD#3 outside the 6-nm bandpass centered at 30 nm were at the detector dark current level (3 pA). The out-of-band currents from PD#1 and PD#3 were more than a factor of 50 smaller than the peak in-band currents (150 pA). This is attributed to the attenuation by the aluminum coatings on the detectors [Fig. 8(b)] and the low grating efficiencies in the higher orders (Fig. 7). On the basis of the ratios of the filter transmittances and the grating efficiencies at wavelengths of 30 nm (first order) and 15 nm (second order), the out-of-band rejection factor is 60 for these two wavelengths.

The spectrometer's field of view was characterized by rotation of the spectrometer in the horizontal

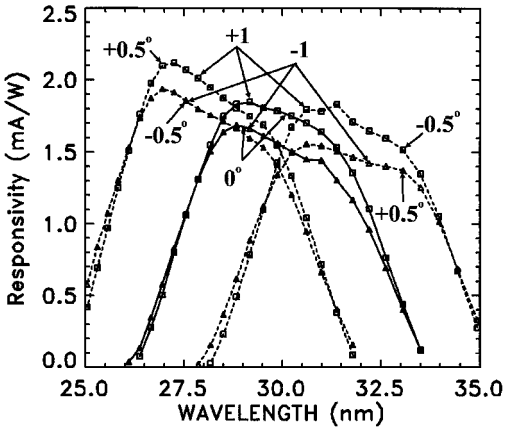

Fig. 10. Responsivities in the +1 and the −1 diffraction orders measured by PD#1 and PD#3, respectively, at the indicated angles of the spectrometer axis with respect to the incident beam.

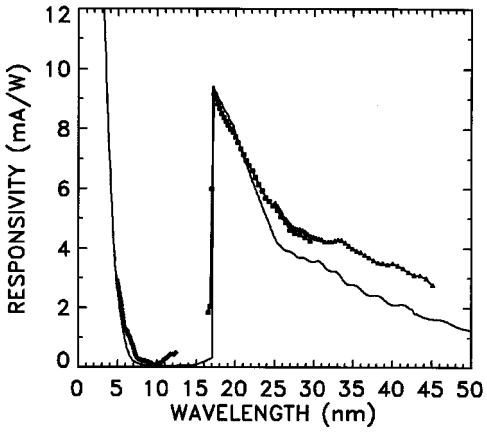

Fig. 11. Measured responsivity in the spectrometer's zero-order channel (data points) and the zero-order responsivity derived from the measured grating efficiency and PD#2 responsivity (curve).

plane about a point centered at the grating. The data for rotation angles of ±0.5°, as well and the data for zero rotation (0°), are shown in Fig. 10. The current ratios were multiplied by the responsivity of the AXUV-100G reference detector.[15] The resulting spectrometer responsivity, the current from the aluminum-coated silicon photodiode detectors divided by the incident radiation power, is shown in Fig. 10.

The detectors' wavelength bandpasses shift with rotation angle in a manner expected from the grating equation. For a rotation angle of 0.5° the wavelength coverage is expected to shift by 1.75 nm. For a given rotation angle the PD#1 (+1 order) and the PD#3 (−1 order) wave bands shift in opposite directions as indicated in Fig. 10. The current from PD#2, which measured the zero-order signal, was insensitive to rotation angle, since the zero order is not dispersed in angle. For angles larger than ±0.5°, the zero-order beam begins to fall outside the area of PD#2.

The measured spectrometer responsivity shown in Fig. 10 is consistent with the measured transmission grating efficiency and the measured transmittance of the aluminum coating on the photodiodes. For example, at a wavelength of 30 nm, the ±1-order efficiency is 2.2% (Fig. 7), and the coating transmittance is 32% (Fig. 9). When we multiply by the AXUV-100G responsivity of 0.22 A/W,[15] the expected spectrometer responsivity is 1.55 mA/W. This may be compared with the value of 1.7 mA/W in Fig. 10 for the case of zero rotational angle at a wavelength of 30 nm. The 9% difference in the two responsivity values is comparable with the expected convolved accuracy of the efficiency and transmittance measurements.

The measurements were performed with normal-incidence, horizontally polarized radiation. Experience with other transmission gratings with 200-nm periods indicates that the grating efficiency should be relatively insensitive to the polarization of the incident radiation in the 30-nm-wavelength region. Modeling indicates that the normal-incidence photodiode responsivity is independent of polarization.[12,18] Thus the spectrometer responsivity is expected to be insensitive to polarization for the case of normal incidence in the 30-nm-wavelength region. The spectrometer mounting in the calibration chamber can be rotated by 90°, so the other polarization can be measured if necessary.

The spectrometer's responsivity in the zero-order channel (PD#2) is shown in Fig. 11. The data points in Fig. 11 represent the measured responsivity, and the continuous curve is the responsivity derived from the product of the measured PD#2 responsivity and the measured zero-order grating efficiency. Figure 11 illustrates the increasing responsivity at wavelengths below 10 nm that, in the case of broadband (e.g., solar) illumination, may produce a significant signal that would add to the signal produced by the bandpass covering wavelengths longer than 17 nm.

6. Discussion

A prototype solar spectrometer consisting of a transmission grating and aluminum-coated silicon photodiode detectors was calibrated with synchrotron radiation. The divergence of the incident radiation beam was ±0.4 mrad in the horizontal direction and ±0.6 mrad in the vertical direction, much smaller than the ±4.4-mrad divergence of solar radiation viewed from Earth orbit. The spectrometer's responsivity in the ±1 diffraction orders at the operating wavelength of 30 nm was 1.7 mA/W. This corresponds to a carrier generation in the external circuit of 0.07 electrons per 30-nm photon that is incident within the spectrometer's field of view.

The shift in the wavelength bandpass with angle of incidence was characterized for angles of ±0.5°, twice the angular size of the solar disk as viewed from Earth orbit. The wavelength dependence of the spectrometer's responsivity is well understood on the basis of the measured grating efficiency, the mea-

sured transmittance of the aluminum coatings on the photodiode detectors, and the angular dispersion of the grating.

The SEM spectrometer on the SOHO spacecraft has measured the solar emission in the 26–34-nm bandpass.[2,3] The emission during periods of minimum and maximum solar activity varied from 1×10^{10} to 3×10^{10} photons/cm^2 s. Much of the emission results from the intense helium II 30.4 nm spectral line. The corresponding power density is 0.65 to 2.0 mW/m^2. Considering the 4 mm $\times$ 10 mm entrance aperture and the 1.7 mA/W responsivity of the presently calibrated spectrometer at a wavelength of 30.4 nm, the solar emission would produce a detector current of approximately 44–136 pA. The addition of a 150-nm-thick aluminum entrance aperture filter would reduce the detector current by a factor of approximately 2.5 to 18–54 pA. By comparison, the detector dark current is 3 pA, is quite steady and can be easily subtracted from the signal.

Part of this research was performed at the National Synchrotron Light Source, which is sponsored by Department of Energy contract DEAC02–76CH00016. We thank J. C. Rife of the Naval Research Laboratory (NRL) for facilitating the synchrotron measurements.

References

1. H. S. Ogawa, D. R. McMullin, D. L. Judge, and R. Korde, "Normal incidence spectrophotometer with high-density transmission grating technology and high-efficiency silicon photodiodes for absolute solar extreme-ultraviolet irradiance measurements," Opt. Eng. **32,** 3121–3125 (1993).
2. D. L. Judge, D. R. McMullin, H. S. Ogawa, D. Hovestadt, B. Klecker, M. Hilchenbach, E. Möbius, L. R. Canfield, R. E. Vest, R. Watts, C. Tarrio, M. Kühne, and P. Wurz, "First solar EUV irradiances obtained from SOHO by the CELIAS/SEM," Sol. Phys. **177,** 161–173 (1998).
3. D. L. Judge, D. R. McMullin, and H. S. Ogawa, "Absolute solar 30.4 nm flux from sounding rocket observations during the solar cycle 23 minimum," J. Geophys. Res. **104,** 28321–28324 (1999).
4. R. Korde and J. Geist, "Quantum efficiency of silicon photodiodes," Appl. Opt. **26,** 5284–5290 (1987).
5. L. R. Canfield, J. Kerner, and R. Korde, "Stability and quantum efficiency performance of silicon photodiode detectors in the far ultraviolet," Appl. Opt. **28,** 3940–3943 (1989).
6. R. Korde, J. S. Cable, and L. R. Canfield, "One gigarad passivating nitrided oxides for 100% internal quantum efficiency silicon photodiodes," IEEE Trans. Nucl. Sci. **40,** 1655–1659 (1993).
7. H. O. Funsten, D. M. Suszcynsky, S. M. Ritzau, and R. Korde, "Response of 100% internal quantum efficiency silicon photodiodes to 200 eV–40 keV electrons," IEEE Trans. Nucl. Sci. **44,** 2561–2565 (1997).
8. L. R. Canfield, "Photodiode detectors," in *Vacuum Ultraviolet Spectroscopy II*, J. A. R. Samson and D. L. Ederer, eds. (Academic, San Diego, Calif., 1998).
9. F. Scholze, H. Rabus, and G. Ulm, "Measurement of the mean electron–hole pair creation energy in crystalline silicon for photons in the 50–1500 eV spectral range," Appl. Phys. Lett. **69,** 2974–2976 (1996).
10. F. Scholze, H. Rabus, and G. Ulm, "Spectral responsivity of silicon photodiodes: high-accuracy measurement and improved self calibration in the soft x-ray spectral range," in *EUV, X-Ray, and Gamma-Ray Instrumentation for Astronomy VII*, O. H. Siegmund and M. A. Gummin, eds., Proc. SPIE **2808,** 534–543 (1996).
11. E. M. Gullikson, R. Korde, L. R. Canfield, and R. E. Vest, "Stable silicon photodiodes for absolute intensity measurements in the VUV and soft x-ray regions," J. Electron Spectrosc. Relat. Phenom. **80,** 313–316 (1996).
12. J. F. Seely, "Responsivity model for a silicon photodiode in the extreme ultraviolet," in *Instrumentation for UV/EUV Astronomy and Solar Missions,* S. Fineschi, C. M. Korendyke, O. H. W. Siegmund, and B. E. Woodgate, eds., Proc. SPIE **4139,** 1–7 (2000).
13. W. R. Hunter and J. C. Rife, "An ultrahigh vacuum reflectometer/goniometer for use with synchrotron radiation," Nucl. Instrum. Methods Phys. Res. A **246,** 465–468 (1986).
14. J. C. Rife, H. R. Sadeghi, and W. R. Hunter, "Upgrades and recent performance of the grating/crystal monochromator," Rev. Sci. Instrum. **60,** 2064–2067 (1989).
15. R. Vest, Electron and Optical Physics Division, National Institutes of Standards and Technology (personal communication, 1999).
16. M. L. Schattenburg, R. J. Aucoin, R. C. Fleming, I. Plotnik, J. Porter, and H. I. Smith, "Fabrication of high energy x-ray transmission gratings for AXAF," in *EUV, X-Ray, and Gamma-Ray Instrumentation for Astronomy V*, O. H. Siegmund and J. V. Vallerga, eds., Proc. SPIE **2280,** 181–190 (1994).
17. M. M. Balkey, E. E. Scime, M. L. Schattenburg, and J. van Beek, "Effects of gap width on vacuum-ultraviolet transmission through submicrometer-period, freestanding transmission gratings," Appl. Opt. **37,** 5087–5092 (1998).
18. J. F. Seely, R. S. Korde, F. A. Hanser, J. Wise, G. E. Holland, J. Weaver, and J. C. Rife, "Characterization of silicon photodiode detectors with multilayer filter coatings for 17 to 150 Å," in *Ultraviolet and X-Ray Detection, Spectroscopy, and Polarimetry III,* S. Fineschi, B. E. Woodgate, and R. A. Kimble, eds., Proc. SPIE **3764,** 103–109 (1999).
19. E. D. Palik, "*Handbook of Optical Constants of Solids* (Academic, New York, 1985).
20. B. L. Henke, E. M. Gullikson, and J. C. Davis, "X-ray interactions: photoabsorption, scattering, transmission, and reflection at E = 50–30,000 eV, Z = 1–92," At. Data Nucl. Data Tables **54,** 181–342 (1993). Updated optical constants were obtained from the following URL: http://cindy.lbl.gov/optical_constants.